Accepted Manuscript

Simultaneous observation of lightning emission in different wave ranges of electromagnetic spectrum in Tien Shan mountains

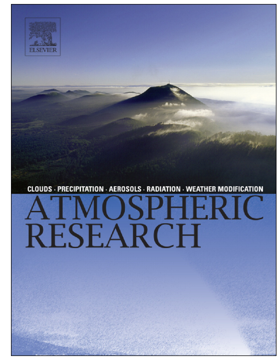

A.V. Gurevich, G.K. Garipov, A.M. Almenova, V.P. Antonova, A.P. Chubenko, O.A. Kalikulov, A.N. Karashtin, O.N. Kryakunova, V.Yu. Lutsenko, G.G. Mitko, K.M. Mukashev, R.A. Nam, N.F. Nikolaevsky, V.I. Osedlo, M.I. Panasyuk, M.O. Ptitsyn, V.V. Piscal, V.A. Ryabov, N.O. Saduev, T.Kh. Sadykov, K.Yu. Saleev, N.M. Salikhov, A.L. Shepetov, Yu.V. Shlyugaev, S.I. Svertilov, L.I. Vil'danova, N.N. Zastrozhnova, Z.S. Zhantaev, K.S. Zhilchenko, V.V. Zhukov, K.P. Zybin

PII:	S0169-8095(17)31239-5
DOI:	doi:10.1016/j.atmosres.2018.04.018
Reference:	ATMOS 4238
To appear in:	*Atmospheric Research*
Received date:	27 November 2017
Revised date:	19 April 2018
Accepted date:	24 April 2018

Please cite this article as: A.V. Gurevich, G.K. Garipov, A.M. Almenova, V.P. Antonova, A.P. Chubenko, O.A. Kalikulov, A.N. Karashtin, O.N. Kryakunova, V.Yu. Lutsenko, G.G. Mitko, K.M. Mukashev, R.A. Nam, N.F. Nikolaevsky, V.I. Osedlo, M.I. Panasyuk, M.O. Ptitsyn, V.V. Piscal, V.A. Ryabov, N.O. Saduev, T.Kh. Sadykov, K.Yu. Saleev, N.M. Salikhov, A.L. Shepetov, Yu.V. Shlyugaev, S.I. Svertilov, L.I. Vil'danova, N.N. Zastrozhnova, Z.S. Zhantaev, K.S. Zhilchenko, V.V. Zhukov, K.P. Zybin , Simultaneous observation of lightning emission in different wave ranges of electromagnetic spectrum in Tien Shan mountains. The address for the corresponding author was captured as affiliation for all authors. Please check if appropriate. Atmos(2017), doi:10.1016/j.atmosres.2018.04.018

Simultaneous observation of lightning emission in different wave ranges of electromagnetic spectrum in Tien Shan mountains

A. V. Gurevich[1,*] alex@lpi.ru, G. K. Garipov[2], A. M. Almenova[3], V. P. Antonova[4], A. P. Chubenko[1], O. A. Kalikulov[5], A. N. Karashtin[6], O. N. Kryakunova[4], V. Yu. Lutsenko[4], G. G. Mitko[1], K. M. Mukashev[5], R. A. Nam[1], N. F. Nikolaevsky[4], V. I. Osedlo[2], M. I. Panasyuk[2], M. O. Ptitsyn[1], V. V. Piscal[1], V. A. Ryabov[1], N. O. Saduev[5], T. Kh. Sadykov[3], K. Yu. Saleev[2], N. M. Salikhov[4], A. L. Shepetov[1], Yu. V. Shlyugaev[7], S. I. Svertilov[2], L. I. Vil'danova[1], N. N. Zastrozhnova[3], Z. S. Zhantaev[4], K. S. Zhilchenko[2], V. V. Zhukov[1] and K. P. Zybin[1]

[1]P. N. Lebedev Physical Institute of the Russian Academy of Sciences (LPI), Leninsky pr., 53, Moscow, Russia, 119991

[2]D. V. Skobeltsyn Institute of Nuclear Physics of the M. V. Lomonosov Moscow State University, Vorob'yovy Gory, 1, str. 2, Moscow, Russia, 119234

[3]Institute for Physics and Technology, Ibragimova, 11, Almaty, Republic of Kazakhstan, 050032

[4]Institute of Ionosphere, Kamenskoye plato, Almaty, Republic of Kazakhstan, 050020

[5]Institute of Experimental and Theoretical Physics of al-Farabi Kazakh National University, al-Farabi pr., 71, Almaty, Kazakhstan, 050040

[6]Radiophysical Research Institute, Bolshaya Pechyorskaya, str., 25/12a, Nizhny Novgorod, Russia, 603950

[7]Institute of Applied Physics of RAS, Ul'yanova str., 46, Nizhny Novgorod, Russia, 603950

[*]Corresponding author.

Abstract

Simultaneous registration of electromagnetic emission generated by atmospheric lightning discharges in the radio-frequency ($f = 0.1 - 30$ MHz), infrared ($\lambda = 610 - 800$ nm), ultraviolet ($\lambda = 240 - 380$ nm), and in the soft energy gamma-radiation ($E_\gamma = 0.1 - 4$ MeV) ranges of electromagnetic spectrum was made synchronously in mountain conditions with complex detector system of the Tien Shan High-Mountain Cosmic Ray Station. We discuss preliminary results of these measurements and perspectives of future application of the multispectral investigation technique to study of the effects of thunderstorm activity.
Keywords thunderstorm, lightning, optic emission, gamma emission, radio emission *PACS* 07.60.-j, 92.60.hx, 52.80.Mg, 92.60.Pw

1 Introduction

In spite of longstanding observation of the powerful atmospheric electric discharges (lightnings) the complete picture of this sporadic and transitory natural phenomenon still remains unclear (MacGorman and Rust, 1998; Rakov and Uman, 2003; Dwyer and Uman, 2014). Therefore, different aspects of this phenomenon are the subject of intensive modern research, and stimulate the progress in observational methods (Usio et al., 2015; Jesùs et al., 2017). The rocket-triggered lightning are also productively studied (Biagi et al., 2011; Jiang et al., 2013). A whole new direction of research, the high-energy atmospheric physics, has arisen after detection of relativistic electrons, X-ray, and gamma ray glow and bursts connected with thunderstorm events (Dwyer et al., 2012). Lately on, the investigations in this field have shown that the measurements of the lightning electromagnetic radiation in a wide frequency range as well as observations of high-energy particle fluxes should be made simultaneously to elucidate the underlying physical processes. Recent examples of such an approach can be found both in TGF studies (Gjesteland et al., 2018) and in the studies of lightning itself (Wang et al, 2018).

In complex investigations which were held at the Tien Shan High-Mountain Cosmic-Ray Station it was found that thunderstorm events can be accompanied by generation of the flow of accelerated electrons, gamma rays and neutrons (Gurevich et al., 2004, 2009, 2011, 2012, 2013; Mitko et al., 2013; Gurevich et al., 2015, 2016). Excess fluxes of energetic particles in storm time which have been called as thunderstorm ground enhancements (TGE) were observed also in a series of analogous experiments made primarily at the Mt Aragats in Armenia (Chilingarian et al., 2011, 2012,, 2015, 2016, 2017), and at other both high altitude (Khaerdinov et al., 2005; Tsuchiya et al., 2012) and sea level (Kozlov et al., 2015; Ishtiaq et al., 2016) sites. Among all emission types, the photons of electromagnetic radiation seem to be most promising as information messengers on phenomena which develop at the time of lightning initiation since they are abundantly generated in this process, and being electrically neutral they can reach rather significant distances from discharge region. The latter circumstance considerably simplifies their detection from the technical point of view.

Experimental attempts to study atmospheric discharge by its optic luminosity have a rather long history and can be traced back up to the early work (Brook, 1960) where a photomultiplier tube was applied to make a counter for nocturnal lightning events. Recent experiments in this field use the modern high-speed video camera (Lu et al., 2009; Kong et al., 2015; Stolzenburg et al., 2016) or fast photodiode (Wilkes et al., 2016) based technique in conjunction with precise electric field sensors and lightning position radars. Primarily, the subject of these experiments is investigation of the initial stage of discharge development with high temporal resolution which permits to discriminate between various possible mechanisms of lightning initiation, the study of the differences between the properties of inter-cloud and cloud-to-ground discharges, the search for peculiar features of candidate discharges which could be the source of giant terrestrial gamma radiation flashes (TGF) in upper atmosphere etc.

In latter experiments it was found that just in the first milliseconds after beginning of a lightning discharge some unexpected flashes of optic light can be observed which coincide with bipolar pulses of the electric field variation. Successive series of such flashes are typical for the process of lightning initiation, they can be found both in cloud-to-ground and cloud-to-cloud discharges. In many cases the succeeding flashes have been seen far apart from the leading one during the first 100–200 μs, than the linear lightning segment has dimmed, and then the whole flash sequence repeated itself on the same path. The visible spatial speed of these primary leaders is very high, it occurs up to $2 \cdot 10^6$ m·s^{-1} during a few first hundreds of microseconds and than it diminishes gradually. Hence, the whole picture of discharge at initial stage of the lightning is much more complicated than it was considered before. In particular, there is still an open question if energetic particles and high-energy radiation do primarily influence the lighting process or they arise only as a byproduct of the latter? To elucidate the physics of atmospheric discharge development the further complex investigations are necessary which should consist of simultaneous registration of electric field, wide band radio emission, gamma ray and optic radiation at the primary stage of a lightning and in a search of mutual correlations in these data.

Presently, we attempt to detect the electromagnetic radiation generated by lightning with radio, optic, and gamma ray detectors simultaneously to test the capabilities of multispectral investigation method in its application to the study of various kinds of lightning discharge. In contrast to mentioned experiments the main goal of our investigation is to search for common features between the remote discharges which can be observed at a large distance by their optic and radio emission only, and the nearby lightning events which occur in close vicinity to detector, and permit to trace the development of particles avalanche immediately by its gamma ray and electron signal.

In thunderstorm season of the year 2016 we made an experiment on synchronous recording of the electromagnetic radiation emitted by atmospheric lightning discharges in near ultraviolet(λ = 240 − 380 nm), visual red and near infrared (λ = 610 − 800 nm), and in a wide (0.1–30 MHz) radio frequency wave ranges. As well, an attempt was made to trace the intensity of soft 0.1–4 MeV gamma-radiation together with observed optic and radio flashes. The measurements were held during the dark time of the days at the detector site of Tien-Shan mountain cosmic ray station (geographical coordinates 43°N, 76°W, the height 3340 m above the sea level; a comprehensive review of the current state of Tien Shan thunderstorm detector complex can be found in (Gurevich et al., 2016)). Preliminary results of this multispectral observation approach of lightning emission are the subject of present paper, as well as discussion of the perspectives which the newly obtained experience in optic signal registration technique opens for the next stage of our thunderstorm investigation activity.

2 Instrumentation

The Tien Shan High-Mountain Cosmic-Ray Station of the P.N. Lebedev Physical Institute is a unique site for investigation of the physics of thunderstorm discharge as well as assumed relationship between the atmospheric and cosmic-ray physics. Its ”Thunderstorm” installation is designed for systematical study of atmospheric discharges and for simultaneous recording of the different types of emitted signals: the electron and neutron radiation components, the gamma, X-ray, optic, and radio radiation, the quasi-static electric field, the acoustic signal. During thunderstorm season (May-September), all the detectors of Tien Shan installation operate continuously in automatic mode. An important advantage of this detector system is its disposition in the altitude range between 3340 and 4000 m above the sea level, just at the height where the thunderstorm clouds are formed in the mountains of Northern Tien Shan, so the detectors occur to be immersed within the clouds by thunderstorm.

2.1 The optic radiation detector

In thunderstorm observation season of the year 2016 the light emittance of atmospheric electric discharges was studied at Tien Shan mountain station with a two-channel lightning radiation detector of the same type as it has been used earlier by Tatiana, Tatiana-2, and Chibis small satellite missions of the Moscow State University (Garipov et al., 2005, 2006; Zelenyi et al., 2014). Detector is based on a pair of Hamamatsu type R1463 photomultiplier tubes (PMT) with multialkali cathode and ultraviolet glass entrance window. The windows of both PMTs are covered with different optic filters: the near visual ultraviolet (UV) range filter of UVS2 type, and the red and near visual infrared light KS11 type filter. The passband of former filter is restricted within the limits of $\lambda = 240 - 380$ nm, while that of the latter is about 610–800 nm (for shortness sake, the second wavelength range herein will be designated simply as ”infrared”, IR). The quantum efficiency of PMT photocathode is of the order of 20%, and nearly uniform within its UV sensitivity window, but it decreases rapidly in the IR range (the efficiency is about 6% at $\lambda \sim 600$ nm, and only about 1% at 800 nm). Above the filters, the PMTs are shuttered with additional 2 mm thick collimator plates which limit the fields of vision within 20° cone at the half height level of their directional pattern, and within 40° cone at the level of 0.1. The fields of vision of both PMTs coincide with each other. Due to the features of local relief, the whole detector set-up is installed at the level of Tien Shan station with its optic axis inclined under $\sim 30^{\circ}$ zenith angle towards northern horizon side, and the free passage of the skylight is opened in measurement times to its entrance windows without any additional light absorber neither scatterer.

Automatic gain control system which is in-built into optic detector regulates constantly the feeding voltage of both PMTs by such a way to keep their anode current at a standard constant level which does not exceed the limit recommended by manufacturer, so the detector can be operating equally well under different conditions in regard to background luminosity of the skylight: both in a dark night when the maximum PMT gain can exceed several millions, and in the evening and morning twilight when the gain falls down to ~ 50. Specific feature of present experiment is that its automatic PMT gain control system keeps track of the PMT anode current in the UV channel only, and varies the feeding voltage of both PMTs inversely to the intensity of sky background in ultraviolet spectrum range. Hence, the background of IR channel is measured here relatively to the fixed level of the UV one.

Recording of electric signal which is elaborated at PMT outputs is made with the use of internal 12-bit analogue-to-digital conversion (ADC) channels of a STM32F407 type microcontroller unit (MCU). Embedded control program which drives the MCU operation provides possibility to measure simultaneously the 20 μs and 190 μs resolution waveforms of its input signal, and to register continuous history of signal behaviour with total duration correspondingly of 0.2 s and about 6 s in both cases. Immediately after registration, the resulting measurements of signal amplitude are kept in a circular buffer within the internal memory of MCU, and as a lightning discharge occurs in vicinity to detector, the time series stored there can be transmitted as a single chunk of data into general database. The proper time for data output is notified to MCU by a trigger signal which is generated at the moment of nearby lightning discharge by special electronic unit (see below). Together with this *external* trigger, the embedded control code of MCU can initiate the data output by itself in any arbitrary moment if the currently measured signal amplitude in either channel exceeds some predefined threshold code. Such *internal* triggering scheme is useful in the case of remote atmospheric discharges when the optic photons in the night time can achieve the detector system from significant distances (some tens or hundreds of kilometers), while the lightning trigger system occurs inactive.

Besides the time series of signal amplitude with microsecond order resolution which are tied strictly to the lightning discharge moment, the MCU control program provides the uniform measurement of the mean amplitude without binding to any specific trigger event. Average amplitudes are calculated continuously by MCU and written automatically with one second periodicity into separate data file. These *monitoring* type data can be used both for stability check of PMT operation in the channels of optic detector, and for tracing the long-term trends in the background luminosity of the night sky.

2.2 The lightning radio-emission

The radio detector system which is used at Tien Shan station as a receiver of radio emission from lightning discharges is described in (Karashtin et al., 2005). It consists of a number of antennae sets spread over the territory of the station. The system is sensitive to electromagnetic emission in a wide frequency range from 0.1 MHz up to 30 MHz, and allows for continuous recording of signal waveforms with 20 ns resolution on a 0.6 s long time space.

Each detector point in considered radio system contains three individual antennas: two mutually perpendicular loop antennas for the measurement of horizontal magnetic field, and a pole end-fed antenna to measure the vertical electric field. All three antennas are the active ones, and include high frequency transistor amplifiers in their set-ups. The use of active antennas allowed us to reduce essentially the overall size of detector assembly, and to reach uniform gain-to-frequency characteristics for all antennas in a wide frequency range. Since the whole apparatus is aimed to operation just in thunderstorm time, special attention was paid to its protection against the damage from the side of nearby lightning discharges. Amplifier outputs from all antenna assemblies are connected to central receiver unit by coaxial cables of equal lengths. The central unit makes it possible to select of up to 4 receiving elements (antennas) which prove to be most suitable for any specific experiment, and to switch their signal to the data recording equipment.

Two antenna sets of considered type are used in the present work. The signal of one of them is written within ±0.3 s time period around the lightning, and is kept in a digital time series form to trace precisely the temporal development history of atmospheric discharge. Another antenna assembly provides the input signal to discriminator unit which generates a short rectangular pulse in the moment when the current amplitude of detected radio-signal exceeds some predefined threshold; typically, this is the situation which occurs just in the moment of nearby atmospheric discharge in thunderclouds. It is this electric pulse from discriminator threshold scheme which is used as a trigger to mark the moment of close lightning discharge, and it is transmitted to all registration subsystems of considered experiment for synchronization of waveform recording. Amplitude threshold of trigger discriminator is deliberately made rather high to avoid detection of random electromagnetic interferences, broadcasting radio-signals and other side effects. Effective generation of lightning trigger is possible if an atmospheric discharge occurs in a rather tight distance range from the antenna location point, up to 3–5 km only.

2.3 The hard electromagnetic radiation

Registration technique for ∼30 keV–10 MeV gamma-radiation from the rainfalls and thunderstorm activity has been developed continuously at the Tien Shan mountain station during the last decades (Chubenko et al., 2009; Gurevich et al., 2009, 2011, 2013). In present work we apply a low-energy gamma-ray detector which is build on the basis of an inorganic scintillator coupled with a FEU49 type PMT. The NaI(Tl) scintillation crystal used as a part of this detector is of 110 mm×110 mm cylindrical form. Together with its photomultiplier and the pulse shaping analogue electronics the scintillator is placed within a solid electrically grounded aluminum casing with a 1 mm wall thickness. Since the end of July 2016, i.e. in the second half of that thunderstorm investigation season, this gamma-ray detector was continuously operating near the top of neighbouring mount in vicinity to Tien Shan station, at a height of ∼400 m above the mean location level of the optic and radio emission detectors. An elevated position was selected to settle the detector possibly closer to generation source of hard radiation in active region of thunderclouds, and to reduce as far as possible the influence of a rather intensive absorption of gamma radiation in the air. To avoid the strong electromagnetic interferences on registration apparatus from close lightnings which are generally typical for such operation conditions, the scintillation detector and all necessary electronics as a whole are placed additionally inside a solid shielding box made of 1 mm thick welded iron, and have an autonomous accumulator based electric source which permits for its continuous operation in storm time independently on any external connection cables.

The registration efficiency of considered detector was defined through complete simulation of the gamma-ray interaction processes inside its scintillator crystal which was made with the use of Geant4 toolkit (Geant4 Collaboration, 2003). The result of this simulation is shown in figure 1 as a dependence of the probability ϵ of any particular gamma ray quantum to be registered by scintillator on its energy. A rather high efficiency of gamma ray registration somewhat compensates the comparatively low aperture of scintillation detector.

More comprehensive description of the hard radiation detectors system currently used at Tien Shan mountain station is made in (Gurevich et al., 2016).

The way of scintillation signal operation is similar to that of the optic detector. Electric pulse from PMT anode, with an amplitude proportional to the energy of detected gamma-quantum, comes to a set of pulse discriminators with increasing operation thresholds. In the time of present experiment up to 12 amplitude discriminators were used simultaneously with their thresholds equivalent to variation of gamma-radiation energy in the limits of 80–2000 keV. The standard digital pulses from discriminator outputs come to the input port pins of a STM32F407 microcontroller unit. In this case, the MCU is driven by a modified embedded program which permits counting of separate pulses at its input instead of former ADC functionality. The measurement of scintillations counting rate is held quite analogously to the optic signal: there are time series of signal intensity taken with resolution of 20 and 160 μs, as well as one second resolution data of uninterruptable intensity monitoring. Since it is essential to avoid any outside cable connections in distant detector point which hosts the hard radiation detector, the MCU operates without switching to any external trigger. Instead, the time series accumulated primarily within the internal memory of MCU can be transmitted for permanent recording directly by MCU own initiative in any moment when the sum multiplicity of input pulses in some scintillation energy channel currently surpasses a predefined threshold over a short time window. This functionality is provided by a special module inside the MCU embedded program. The energy channel used for generation of this internal trigger event, so as concrete threshold number of registered pulses and duration of the time window were selected by practical experience, and deliberately made permissive enough as a tradeoff between a sufficiently high probability of event registration in the case of any transient radiation intensity increase because of nearby atmospheric discharge, and a tolerable amount of background ”noise” events from the false positive realizations of trigger condition in arbitrary times.

2.4 Electric field and acoustic measurements

In thunderstorm time the local quasi-static near-Earth electric field at the site of Tien Shan mountain station is measured with a special ”field-mill” type sensor which is installed in vicinity to optic luminosity detector. Electric field sensor used for this purpose is made *ad exemplum* of the standard EFM-100 type field detector of Boltek production (Boltek, 2016). The sensor contains a pair of disk electrodes installed one above the other with a small spatial gap between. One of these electrodes is connected to ground potential and is kept rotating with constant speed. There are four holes made in rotating electrode, while another, the fixed one, is divided into 4 quarters which alternately occur either open or shielded by a solid part of the moving disk. Within an electric field, a modulated voltage is induced between the open and shielded parts of the fixed, measuring electrode. Peak amplitude of this voltage is a linear function of external atmospheric field, and its phase depends on the sign of the latter. The control signal to phase detector comes from an optic sensor, with light flux modulated by a cog-wheel mounted on the axis of the motor which drives the movable electrode. With four holes in grounded electrode which moves with the speed of 50 rotations per second, the frequency of pulse signal after phase detector is about 200 Hz. A low pass filter installed at its output has the cutoff frequency of 10 Hz. Hence, the time resolution of the field-mill sensor is about 100 milliseconds only. Despite this slowness, an incontestable merit of the field mill detector type is the possibility of absolute calibration of its indications, immediately in the units of the field magnitude.

Another kind of field detectors applied at Tien Shan station is an electric field change (E-change) sensor which consists of a 0.5×0.5 m^2 flat capacitor with one of its plates being grounded, and the other one exposed freely to the influence of environmental field. The fast variable voltage pulse which is induced between these plates in the moments of nearby atmospheric discharges is digitized in parallel with the field mill signal, i.e. with the same 190 μs temporal resolution. Hence, the limit frequency of E-change type measurements in present experiment is about 2.5 kHz.

A number of sensitive microphones installed in different points on the territory of Tien Shan station permit to measure the time of thunder sound delay relative to lightning trigger. In the case of close lightnings (up to 7–10 km) this information is useful to estimate the distance to discharge region, and to locate roughly its position through comparison of mutual time delays between the arrival moments of thunder sound in spatially separated points.

3 Results and discussion

3.1 Low-resolution monitoring data of radiation intensity

Figure 2 presents the typical low-resolution records of the average intensity of optic radiation, and of the magnitude of local electric field as both are seen at the fair weather time (top plot panels), and in thunderstorm period. All distributions were recorded continuously with one second time periodicity during the dark time of the day (in the season of measurements, the moment about 15h UT corresponds to beginning of the night, and the time after 22h UT—to morning twilight before sunrise at the longitude of Tien Shan station). Ordinate axes of the plots of optic signal are graduated immediately in the units of 12-bit codes which result after amplitude conversion (the maximum possible value is 4095).

It was found that during dark moonless nights and in absence of any close thunderstorm passage the intensity monitoring records of optic radiation generally have a rather smooth form without any sharp outbursts, with their mean amplitude oscillating around the code level of ∼30–40, like the cases shown in upper row of the plots in figure 2. In such conditions, the optic detector can rarely register (thanks to its internal autonomous trigger facility) only the weak flashes of radiation which have been born by remote lightnings at the distances of some tens of kilometers at least, and later on the optic light was scattered and reflected towards detector by the high-altitude clouds in upper atmosphere.

Contrary to this, if a close passage of some nighttime thunderstorm at a distance of 1–3 km from detector system reveals itself by a sharp and fast variation of electric field (and through an evident time delay between the lightning flash and thunder sound), the records of optic signal both in IR and UV wave ranges demonstrate the presence of multiple narrow irregularities with peak ADC amplitude of the order of some hundreds which usually coincide with the moments of abrupt, extremely intensive changes in the magnitude of electric field. Example records of this kind are shown for the dates of 2 and 17 July 2016 in lower panels of the figure 2. Typical duration of these outbursts does not exceed the length of a single measurement, i.e. it is below 1 s, so the registered luminosity flashes are evidently connected with atmospheric discharges which can be traced through abrupt synchronous changes in the mean magnitude of the local electric field.

3.2 Transient optic flashes around the moment of atmospheric discharge

A sample of 190 μs resolution time series of the intensity of IR and UV optic flash from a lightning written together with its radio frequency signal is presented in figure 3. The radio and optic distributions in these events have been synchronized by the same lightning trigger from the radio antenna set. Usually, this trigger coincides with the first radio pulse of the sequence of discharges that the lightning process consists of whose amplitude occurs above the discriminator threshold. Because of a high threshold level the ’trigger’ pulse will not always be the leading one in this sequence, but since the whole time series of signal measurements is kept both before and after the trigger the history of lightning development can be traced completely, though sometimes with a shift into negative region of the time axis.

The case most commonly met in such kind of events is shown in the top left panel of this figure (the event of 17 July 2016, 19:12:21 UT). Complete history of discharge development here can be traced precisely by momentary amplitude of radio signal which typically consists of a series of intensive short-time outbursts with duration of the order of some units or tens of microseconds, separated by millisecond-long gaps where its intensity is negligible. As shown in (Karashtin et al., 2005) and (Gurevich and Karashtin, 2013), this type of transient radio bursts is generated immediately within the active discharge area by development of succeeding streamer processes in atmosphere. As a role, every peak of radio emission from elementary streamer is accompanied with an abrupt momentary variation in potential of the local electric field, which can be traced by the fast signal of capacitor type E-change detector. The slow variation trend of the mean local field in nearby environment which goes on over the whole discharge time is illustrated by indications of the field mill sensor in bottom plot of this panel.

It is seen in considered event of 17 July 2016, 19:12:21 UT that the optic flashes in both spectrum ranges usually occur to be quite synchronous, and every IR peak has its UV counterpart with comparable measured amplitude. Taking into account the significant difference in quantum efficiency of PMT photocathode in both spectrum ranges, it can be stated that in fact the amplitude of IR signal (which is proportional to radiation intensity in this wave range) is an order of magnitude higher than that of UV pulse. It should be noted also that the observed signal amplitudes in our measurements are limited from above by a threshold which corresponds to ADC code about 3700–3900, because of saturation of analogue circuits in electronic channels of optic detector. As well, it can be seen a remarkable synchronism in considered event between transient IR and UV flashes on the one hand, and narrow radio and fast E-change signals from succeeding discharges on the other which makes all these signals practically coinciding on the time scale of the plot. Similar strict connection between the moments of abrupt changes in the magnitude of electric field and (somewhat delayed) short-time flashes of visible luminosity by lightning development was reported in the studies (Wilkes et al., 2016; Stolzenburg et al., 2016) which have been made with better temporal resolution.

Time behaviour of optic emission both in IR and UV ranges usually follows strictly to that of the radio signal, but the fine peculiarities of their intensity profile are distinctly different. The flashes in optic range of electromagnetic spectrum occur to be much smoother than the radio ones, which effect can be explained by diffuse scattering of optic photons within thunderclouds, and by significant dispersion of their trajectories and time delays on the path from emitting area to detector system. Both these effects result in smoothing and stretching of the sum IR and UV pulses in observation point. Nevertheless, it is seen that all short, sub-millisecond long radio pulses in considered event are accompanied by transient optic flashes which have nearly same duration. Hence, the optic flashes with visible duration of some successive milliseconds which are also present in this event immediately besides the short ones can not result from any peculiarities of light propagation in the clouds, but must originate from the discharges of some different (prolonged) kind which in fact last continuously over the time of millisecond order.

In similar lightning event presented in the top right panel of figure 3 (25 July 2016, 14:04:27 UT) any significant optic radiation is evidently absent during the whole beginning part of electric discharge which can be clearly traced by its radio emission. Comparatively weak optic signal starts to be seen only after a ~300 ms long delay since the beginning of discharge development. The absence of noticeable optic flash in this case can be possibly explained either by low generation efficiency of optic photons at initial stage of discharge, or by anomalously high absorption of the light in thunderclouds at the point of discharge initiation. Quite an opposite case is seen in the left bottom panel of figure 3, where the UV radiation intensity resolutely prevails above that of IR signal. Similar picture is seen in the case of 5 July 2016, 14:34:59 UT event which is shown in the right bottom panel of figure 3. Here, there is no visible optic signal at the moment of leading atmospheric discharge observed accordingly to its radio emission, then an optic flash reveals itself only in UV frequency range at the second prominent radio pulse, and then the characteristic lightning imprint is seen simultaneously in both optic signals. Observation of familiar lightning imprint at the end of considered event means the absence of any anomalous light absorption in the clouds, so unusual peculiarities in distribution of the intensity of optic flash in this case are in fact caused by unequal efficiency of light generation in corresponding parts of electromagnetic spectrum at initiation moment of the different ”dark” and ”bright” types of atmospheric electric discharge.

It should be noted that the duration of transient luminosity flashes considered above (which are of micro- and millisecond order) is much shorter than characteristic reaction time of the circuitry of PMT gain control (some minutes), so the latter can not make any influence on recorded time series of IR and UV signal, and can not be the reason of their difference from the radio and E-change data records. A rather large time gaps between succeeding atmospheric discharges (typically, about some tens of seconds) permit to conclude that the probability of any accidental overlap between neighbouring discharge events on a same time series is too negligible to be accountable for this effect also.

As well, intensive scattering of optic radiation in the clouds which is typical for thunderstorm weather eliminates effectively any influence of the limited field of vision of our optic sensor. Usually, the lightning illuminates quite uniformly the whole hemisphere of the night sky, so we observe not a lightning image itself but a transient flash of scattered optic radiation above the sky background. Such illumination of surrounding clouds which are much greater than the source of radiation itself can be seen immediately on the high-speed video images of lightning development in the work (Stolzenburg et al., 2016). It is especially noted there that the scattered luminosity signal can reach the detector from the large regions deeply immersed in the clouds. Hence, any restriction in direct field of vision of applied optic detector can not be responsible for the said fine features in behaviour of the radio, IR, and UV signals, and the mutual differences of the latter are indeed a real effect.

Spectral peculiarities of optic emission from atmospheric discharges were considered in modelling work (Dwyer et al., 2013). An existence of some specific discharge types, such as ”purplish-blue” (300–400 nm) and ”dark” lightnings is mentioned there which conclusions agree with direct observations of spectrum differences in present study. It should be noted that from an experimenter’s point of view the difference in relative energy distribution between IR, UV, and radio signal opens an opportunity for selection physically different kinds of discharge events through realization of specific trigger conditions at the night time. Hence, the technique of optic signal registration occurs to be complimentary to the one based on registration of the radio emission only which so far has been used traditionally in Tien Shan experiments.

The relative durations of the optical emission and the variations in the local electric field in a typical lightning event are compared in the figure 4. The electric field changes start with a sharp dip into negative values immediately before the beginning of visible lightning, followed by a rather prolonged exponential restoration of the mean field magnitude to its initial zero level which takes many seconds. As well, the record of acoustic signal on the bottom plot of this figure illustrates the arrival of thunder sound with time delay of 3.5–4 s, which corresponds to linear distance to discharge region of about 1 km in this rather close lightning event.

3.3 Distant discharge events with an optic flash trigger

Internal triggering facility provided by the MCU embedded program which is used for the control of ADC measurement gives a possibility to register the optic radiation flashes from some rather distant atmospheric discharges when the accepted radio-signal occurs insufficient for reliable generation of event trigger. A sample of a such type of events is presented in the figure 5. It is seen there that the intensity of radiation from some distant but powerful lightnings was quite enough to achieve saturation of electronic PMT channels both of IR and UV ranges. Nevertheless, any trigger signal has not been generated in these events by the radio-antenna sensor, seemingly, because of significant remoteness of discharge and the high threshold of trigger discriminator. The absence of any sign of thunder sound detection in these events permits to conclude that the distance to discharge region was larger than 10 km, where the lightning trigger is ineffective.

Hence, the use of the optic signal registration method together with algorithm of internal trigger elaboration which is bound to some threshold amplitude of registered light widens significantly the sensitivity area of the lightning detector system, and gives a possibility to study precisely the development of remote electric discharges at a great distance, up to some tens of kilometers from detector point. Due to high susceptibility of optic sensor to the scattered lightning emission this possibility remains existing even in a cloudy or misty storm weather. The only necessary factor for applicability of this method is the presence of a sufficiently open field of view around the horizon which condition is agreeably satisfied at the Tien Shan station with its location on a mountain pass.

3.4 20 μs resolution radiation series in the range of discharge beginning

The beginning of a luminous discharge can be traced in more details when applying systematically the 20 μs resolution time series of the optic amplitude measurements. An example of such type of events is presented by the plots in upper row of figure 6, where much more abundant multitude of narrow features in the time distribution of flash intensity can be found than in the plots of figure 3. Here, again, the use of IR and UV signal for the study of lightning development in the night time can be more favorable from the viewpoint of registered events statistics in comparison with radio emission based trigger, due to large distribution area of the scattered optic photons.

As well as the lightning flashes which usually last some prolonged time, of the order of tens and hundreds of milliseconds, intensity measurements with enhanced time resolution permit to observe in detail a very short radiation bursts of much smaller, sub-millisecond duration. Usually, these are the 0.1–0.5 ms long single peak luminosity flashes, like to sample events shown in the middle row of figure 6. Characteristic features in temporal behaviour of these events are the duration of about some hundreds of microseconds of a separate radiation peak, and its $\sim$50–100 μs delay relative to initiation moment of discharge development which can be seen in synchronous radio-data. These results are in agreement with corresponding values which have been presented in the work (Wilkes et al., 2016) for various kinds of inter-cloud and cloud-to-ground atmospheric discharges.

Besides the events with comparable amplitude both of the infrared and ultraviolet flash it was found another case when radiation has absolutely prevailed only in one of considered wave ranges. This type of events is illustrated by the plots in lower row of the figure 6. Typical feature of these events is decisive predominance of a single spectrum part in their radiation: as a rule, an intensive UV pulse is combined with a very weak or fully absent signal in IR wave range or vice verse. Most frequently met type of these events is a narrow spike-like outburst of UV light, like the one shown in the left bottom panel of the figure 6 but the ”infrared” light flashes can be met also. Usually, such bursts do not exceed the 20 μs duration of a single ADC measurement interval. At the same time, the significant pulse amplitude which achieves often the ADC codes of some hundreds and thousands, means a rather powerful mechanism of light generation in these transient peaks.

3.5 The hard electromagnetic radiation

Figure 7 presents the monitoring type records of the intensity of background gamma-radiation which have been written with one second time resolution during three time periods: in a clear night, when the gamma-ray scintillation detector was operating synchronously with optic and radio ones (the date of 9 August 2016); in stormy night when some remote thundercloud system can be seen by multiple optic flashes of its lightnings far apart at the horizon, at some tens of kilometers distance (26 July 2016; the order of clouds distance >10 km was estimated both by the absence of any thunder sound marks in acoustic detector records, and visually, thanks to a large field of view from elevated position of the Tien Shan station); and in a daylight thunderstorm time when the thunderclouds accompanied with intensive precipitations (rain and hail) were passing immediately above the detector at a few kilometers height. Every plot frame on this figure presents just a set of intensity distributions which have been measured for monotonously increasing energy thresholds of registered gamma-radiation, from 80 keV and up to 3–4 MeV.

It is seen that in a clear night time the background intensity distributions of hard electromagnetic radiation demonstrate the same undisturbed behaviour as the optic records do: they have a rather smooth shape in all registered gamma ray energy ranges without any abrupt excess of radiation amplitude. Such a smooth distribution shape is commonly typical for a quiet weather conditions.

Specific feature of the method of optic emission registration is illustrated by the median frame in figure 7. During this rather stormy night the gamma ray detector at its distant high altitude location point was operating uninterruptedly, and simultaneously with optic sensor. While the latter has registered in the period between ∼15 h and ∼16 h UT a multitude of short intensive outbursts of the scattered optic photons from distant lightnings, there were only some scarce peaks of gamma radiation detected at that night, and in the range with lowest (80 keV) energy threshold only. The high-energy gamma ray distributions during that night occur just as smooth as in any quiet time, which is caused by significant distance between the detector disposition place and the lightning bound source of gamma radiation. It should be noted that in low-threshold series the number of gamma-ray signals detected in transient pulses is an order of magnitude higher than the statistic fluctuations of the background counting rate. Any origination of observed short time peaks from electromagnetic interferences of industrial nature which could be influencing the gamma ray detector operation is quite unlikely since such peaks are totally absent in the fair weather time. As well, any noise interferences should be also detected by the optic sensor whose sensitivity is not worse than that of the gamma one. Hence one can state that in this event we see indeed the flashes of gamma radiation at a larger distances from the lightning region than it was possible before at Tien Shan station with the use of gamma ray and radio detector technique only.

The third, rightmost plot frame in figure 7 demonstrates the usual time behavior of the gamma radiation intensity in the period of close thundercloud passage. Here, again, characteristic transient peaks of low-energy gamma radiation can be seen just at the time when close thunderclouds were moving in detector vicinity. Shortly after the beginning of thunderstorm and its accompanying precipitation, the intensity of environmental gamma ray background starts to grow, and the enhanced radiation level remains existing even after storm termination during a rather long time, of the order of 2–3 hours, decreasing slowly with a constant speed.

Besides this slow trend in the counting rate during the considered daytime thunderstorm, just around the storm moment one can see the short spike-like outbursts of gamma ray intensity in low-threshold distributions. Both the shortness and a rather high amplitude of these bursts are their characteristic features which differ them distinctly from the slow variation. As it was discussed in (Gurevich et al., 2016), the transient gamma bursts are connected with nearby lightning discharges, and correspond to gamma radiation from accelerated particle avalanches which develop inside thundercloud. Because of a number of reasons, such as a limited absorption path of low-energy gamma radiation in atmosphere, and presumably anisotropic angular distribution of emitted gamma rays, effective detection of the gamma ray signal is possible only if an atmospheric discharge occurs in a rather close vicinity of detector system, so the distance from the gamma detector and discharge region does not exceed 1–3 km. In contrast to this, the optic radiation based technique does not have such limitation, and can be applied for investigation of remote lightning events, so both methods are complimentary to each other.

In stormy night period of the date 26 July 2016 an attempt was made to register the high resolution time series of the intensity of hard gamma radiation simultaneously with soft optic emission from the distant lightning discharges, with mutual synchronization of both distributions by the common discharge trigger. A sample of this kind of events is presented in the figure 8. In these measurements the gamma ray intensities were registered as usual, with periodicity of 160 μs, but because of a generally scarce amount of gamma ray signals which reach the detector, every 5 succeeding counts in corresponding time series were additionally summed together to increase the statistics of the points of presented distribution curves, so the resulting time resolution of the gamma radiation data shown in the plots of figure 8 is 800 μs. All distributions are synchronized by internal trigger of the optic detector which corresponds to beginning of the visible flash from the lightning.

In these events, some correlation is seen in position of prominent intensity peaks of the optic and gamma ray distributions. To check it more precisely, the statistical reliability of these peaks was estimated on the basis of the mean background count rates from the figure 7. According to monitoring records, an integral amount of random pulses which could fall accidentally at a single 800 μs long interval in the time series with 80 keV energy threshold is about 2 int^{-1} only, and about 0.5 int^{-1} for the >1900 keV distribution. Hence, the observed peak amplitude about 8–15 int^{-1} in the low threshold time series, and about 4–6 int^{-1} in the high threshold ones correspond to statistically significant level of 3–4σ. It is seen also that the gamma radiation energies in excess short-time peaks which coincide with the flashes of optic emission in figure 8 stretch from keV values up to the $E_\gamma \sim 1\text{–}2$ MeV at least. Similar hard energy spectra of transient gamma radiation bursts which accompany the atmospheric electric discharges were noted in (Gurevich et al., 2016).

It should be stressed that generally the observation conditions of the lightning connected gamma ray signal were rather unfavorable in considered storm night because of a large remoteness of thundercloud system. In particular, there has not been generated any high-threshold trigger from the radio detector which is the reason why the radio signal series are absent in the figure 8. Unfortunately, there has not occurred any close nighttime thundercloud passage during the whole operation period of the gamma ray detector in second half of the 2016 year season, so any detailed high resolution registration of some prominent gamma ray signal from lightning discharge accompanied and strictly synchronized with its radio- and optic emission flash still remains an open task for further investigations at Tien Shan.

Nevertheless, even in this unfavorable case an exceptionally interesting event has been caught which is shown under timestamp of 26 July 2016, 15:45:29 UT in the figure 8. It is seen there how the wide band electromagnetic spectrum radically changes just in the course of this particular radiation flash: only the ultraviolet and gamma-ray quanta have been registered in the beginning part of atmospheric discharge up to a few milliseconds since its initiation moment, while the infrared radiation was virtually absent, than the gamma-ray signal disappears, and the common mixture of UV and IR radiation remains instead as it is usual for conventional discharge type. Hence, the considered event could be interpreted as immediate observation case of the change between the e/γ-avalanche driven and convenient discharge modes in lightning development. Similar luminosity flashes with immediately observed variation in their optic spectra have been detected earlier at satellites in certain regions of the Earth, where the flashes of usual lightnings occurred relatively scarce (Garipov, personal communication). Presumably, the features of atmospheric discharges discussed in the present paper could be due also to specific properties of the Tien Shan region.

3.6 On statistics of the observed events

During 2016 year thunderstorm season at the Tien Shan station it was observed 2158 events with detected optic flashes which have occurred in 32 nighttime storms. Among these optic events, 164 have been recorded together with corresponding radio emission signal, and 14 were accompanied with visible traces of gamma radiation. Here, again, one can see a much higher efficiency of lightning events selection by their optic emission in comparison with traditional radio trigger based technique.

4 Conclusion

Next step in the studies of thunderstorm processes in atmosphere at Tien Shan High-Mountain Cosmic Ray Station is connected with immediate registration of optic radiation emitted at the bright phase of lightning discharge together with its gamma-ray and radio emission. In thunderstorm season of the year 2016 a pair of optic detectors was applied for this purpose, one of them being sensitive to the $\lambda = 610 - 800$ nm red and infrared range photons, and the other one—to ultraviolet radiation ($\lambda = 240 - 380$ nm). During this period some hundreds of optic events have been traced in the nighttime from the lightnings of ∼30 thunderstorms, both remote (with the distance R to active storm region being $\gtrsim 10$ km), and close ($R \lesssim$ 3-5 km) ones. It was found that mostly the development patterns of the infrared and ultraviolet flash from a lightning discharge correlate well, both with each other and with that of the radio emission signal, but a variety of peculiar atmospheric discharge types has been revealed:

- the ”dark” electric discharges without significant optic radiation;
- prolonged continuous optic flashes which last uninterruptedly about some milliseconds and ”fill” the gaps between separate radio pulses from succeeding discharges;
- short-time intensive optic flashes with sub-millisecond duration;
- transient flashes with decisive predominance of UV range radiation in their optic spectrum;
- inversely, the ’red’ flashes with intensive IR signal and the absence of any noticeable ultraviolet radiation.

In a part of 2016 year exposition the optic and radio emission detectors were operating together with a gamma ray detector, and a transient gamma radiation burst signal was seen from a thundery front in the energy range from ∼100 keV and up to ∼2 MeV. The duration of these bursts is about a few milliseconds or shorter, which complies well with typical TGF duration but is much shorter than the TGE.

According to practical experience of the 2016 year thunderstorm season, one can state that the combined use of the radio- and optic electromagnetic emission detectors together with sufficiently high temporal resolution of registered signal (about 10 μs or better) permits to study the development of natural lightnings with sufficiently high precision, which circumstance can play a key role for comparison of various existing theoretical models of atmospheric electric discharge. The possibility to register the time behaviour of the very remote atmospheric discharges, and quite independently on local weather conditions which is specific feature of the optic signal based technique can be rather useful to gain promptly the necessary statistics of observed discharge events.

Acknowledgments

This work was supported by the Programs #I.3, #I.11, and #I.28 of the Russian Academy of Sciences; by the RFBR grant #15-45-02636; by the Scientific-Technical Program ”Development of High-Energy Physics, Cosmic Rays, and its Practical Applications in Kazakhstan Republic for 2015-2017 years”; by the Aerospace Committee of Kazakhstan Republic, as a part of its Targeted Budget Program (O.0674) for the 2015-2017 years (N0115RK01275); by the IRN program #BR05236494 ”Fundamental and applied studies in related fields of physics of terrestrial, near-earth and atmospheric processes and their practical application”; and by the IRN program #BR05236291 ”Perspective fundamental investigations on the physics of cosmic rays and astrophysics at the Tien Shan Mountain Station in the years 2018-2020”.

References

Biagi, C.J. et al., 2011. Observations of the initial, upward-propagating,steps in a rocket-and-wire triggered lightningpositivedischarge leader. Geophys. Res. Lett. 38, L24809.

Boltek Lightning Detection Systems. EFM-100 electric field mill, 2016. http://www.boltek.com/EFM100-SS-09112016.pdf.

M. Brook and N. Kitagawa., 1960. Electric-field changes and the design of lightning-flash counters. J. Geophys. Res., 65(7).1927–1931.

Chilingarian, A., Hovsepyan, G., Hovhannisyan, A., 2011. Particle bursts from thunderclouds: Natural particle accelerators above our heads. Phys. Rev. D 83: 062001.

Chilingarian, A., Bostanjyan, N., Vanyan, L., 2012. Neutron bursts associated with thunderstorms. Phys. Rev. D 85, 085017.

Chilingarian et al., 2012. Recovering of the energy spectra of electrons and gamma rays coming from the thunderclouds. Atm. Res. 114–115, 1–16.

Chilingarian, A. et al., 2017. On the initiation of lightning in thunderclouds. Sci. Rep. 7, 1371–1381.

Chilingarian, A., Chilingaryan, S., Reymers, A., 2015. Atmospheric discharges and particle fluxes. J. Geophys. Res.: Space Phys. 120, 1–9.

Chilingarian, A., Hovsepyan, G., Kozliner, L., 2016. Extensive air showers, lightning, and thunderstorm ground enhancements. Astropart. Phys. 82, 21–35.

Chubenko, A. et al., 2009. Energy spectrum of lightning gamma emission. Phys. Lett. A 373 (39), 2953–2958.

Dwyer, J. R., Uman, M. A., 2014. The physics of lightning. Physics Reports 534 (4), 147–241.

J. R. Dwyer, N. Y. Liu, and H. K. Rassoul., 2013. Properties of the thundercloud discharges responsible for terrestrial gamma-ray flashes. Geophys. Res. Lett. 40, 4067–4073.

Dwyer, J. R., Smith, D. M., Cummer, S. A., 2012. High-energy atmospheric physics: Terrestrial gamma-ray flashes and related phenomena. Space Science Reviews 173 (1), 133–196.

Garipov, G. K. et al., 2005. UV radiation from the atmosphere: Results of the MSU Tatiana satellite measurements. Astropart. Phys. 24, 400–408.

Garipov, G. K. et al., 2006. Ultraviolet radiation detector of the MSU research educational microsatellite *Universitetskii-Tatiyana*. Instrum. Exp. Tech. 49, 126–131.

Garipov, G. K. Personal communication.

Gjesteland T. et al., 2017. On the timing between terrestrial gamma ray flashes, radio atmospherics, and optical lightning emission. J. Geophys Res.: Space Phys. 122 (7), 7734–7741.

Geant4 Collaboration, 2003. Geant4 – a simulation toolkit. Nucl. Instrum. Methods A 506 (3), 250–303.

Gurevich, A.V. et al., 2004. Experimental evidence of giant electron-gamma bursts generated by extensive atmospheric showers in thunderclouds. Phys. Lett. A 325, 389–402.

Gurevich, A. V. et al. 2009a. Nonlinear phenomena in the ionospheric plasma. Effects of cosmic rays and runaway breakdown on thunderstorm discharges. Phys.-Uspekhi 52 (7), 735–745.

Gurevich, A. V. et al., 2009b. An intracloud discharge caused by extensive atmospheric shower. Phys. Lett. A 373 (39), 3550–3553.

Gurevich, A.V. et al., 2011. Gamma-ray emission from thunderstorm discharges. Phys. Lett. A 375 (15), 1619–1625.

Gurevich, A.V. et al., 2012. Strong flux of low-energy neutrons produced by thunderstorm. Phys. Rev. Lett. 108, 125001–4.

Gurevich, A.V., Karashtin, A.N., 2013. Runaway breakdown and hydrometeors in lightning initiation. Phys. Rev. Lett. 110, 185005.

Gurevich, A.V. et al., 2013. Correlation of radio and gamma emissions in lightning initiation. Phys. Rev. Lett. 111, 165001.

Gurevich, A.V. et al., 2015. The time structure of neutron emission during atmospheric discharge. Atmos. Res. 164-165, 339–346.

Gurevich, A.V. et al., 2016. Observations of high-energy radiation during thunderstorms at Tien-Shan. Phys. Rev. D 94, 023003–9.

Ishtiaq, P. M. et al., 2016. Observation of 2.45 MeV neutrons correlated with natural atmospheric lightning discharges by Lead-Free Gulmarg Neutron Monitor. J. Geophys. Res.-Atmos. 121 (2), 692–703.

Lòpez, J.A. et al., 2017. Spatio-temporal dimension of lightning flashes based on three-dimensional Lightning Mapping Array. Atmos. Res. 197, 255–264.

Jiang, R. et al., 2013. Propagating features of upward positive leaders in the initial stage of rocket-triggered lightning. Atmos. Res. 129–130, 90–96.

Karashtin, A. N., Shlyugaev, Y. V., Gurevich, A. V., 2005. High-frequency radio emission of the lightning discharge. Radiophys. Quantum Electron. 48 (9), 711–719.

Khaerdinov, N. S., Lidvansky, A. S., Petkov, V. B., 2005. Cosmic rays and the electric field of thunderclouds: Evidence for acceleration of particles (runaway electrons). Atmos. Res. 76 (1-4), 346–354.

Kong, X. et al., 2015. Optical and electrical characteristics of in-cloud discharge activity and downward leaders in positive cloud-to-ground lightning flashes. Atmos. Res. 160, 28–38.

Kozlov, V. I. et al., 2015. Recording neutrons with 10-μs resolution during a thunderstorm in Yakutsk. Bull. Russ. Acad. Sci. Phys. 79, 685–687.

Lu, W. et al., 2009. Simultaneous optical and electrical observations on the initial processes of altitude-triggered negative lightning. Atm. Res. 91, 353–359.

MacGorman, D.R., Rust, W.D., 1998. The Electrical Nature of Storms. New York: Oxford Univ. Press.

Mitko G.G. et. al., 2013. Bursts of gamma-rays, electrons and low-energy neutrons during thunderstorms at the Tien-Shan. J. Phys.: Conf. Ser., 409. 12235 (5).

Rakov, V. A., Uman, M. A., 2003. Lightning. Physics and Effects. Cambridge: University Press.

Stolzenburg, M. et al., 2016. Luminosity with intracloud-type lightning initial breakdown pulses and terrestrial gamma-ray flash candidates. J. Geophys. Res. Atmos. 121, 919–936.

Tsuchiya, H. et al., 2012. Observation of thundercloud-related gamma rays and neutrons in Tibet. Phys. Rev. D 85, 092006.

Ushio, T., Wu, T., and Yoshida, S., 2015. Review of recent progress in lightning and thunderstorm detection techniques in Asia, Atmos. Res., 154, 89–102.

Wang C. et al., 2018. Characteristics of downward leaders in a cloud-to-ground lightning strike on a lightning rod. Atmos. Res. 203, 246–253.

Wilkes, R.A. et al., 2016. Luminosity in the initial breakdown stage of cloud-to-ground and intracloud lightning. J. Geophys. Res. Atmos. 121, 1236–1247.

Zelenyi, L.M. et al., 2014. The academic Chibis-M microsatellite. Cosmic Res. 52, 87–98.

Figure 1 Energy dependence of registration efficiency of the gamma radiation detector.

Figure 2 Monitoring records of the average optic radiation amplitude, and of the local electric field which have been made with one second periodicity during two quiet (above), and two stormy nights (below). Vertical axes are graduated in the units of 12-bit ADC codes.

Figure 3 A sample of lightning discharge events with synchronous registration of the radio and optic emission together with signal record of the E-change capacitor detector and of the field mill sensor. Temporal series were measured with 190 μs resolution. Zero point of the time axis corresponds to arrival moment of a lightning trigger from the radio antenna set.

Figure 4 The long-scale signal intensity records of a lightning flash event. Zero point of the time axis coincides with lightning trigger from the radio antenna set.

Figure 5 Intensive flashes of optic radiation from the distant atmospheric discharges taken with internal trigger of the ADC facility. Zero point of the time axis corresponds to beginning of the visible optic flash from lightning discharge.

Figure 6 Detailed picture of the beginning stage of lightning discharge development revealed in 20 μs resolution time series of the optic radiation intensity.

Figure 7 Monitoring records of the counting rate of gamma ray pulses N_p which have been obtained in a quiet night (left plot), in a night with observation of a distant thundercloud system (in the middle), and during a typical close thunderstorm passage at the daytime (right plot). Time resolution is 1 s.

Figure 8 A sample of simultaneously written high resolution series of the intensity of lightning emission in the infrared, ultraviolet, and gamma ray ranges of electromagnetic spectrum.

Highlights

- Different atmospheric discharge emissions were investigated simultaneously.
- Modified set of equipment was used at Tien-Shan Station during thunderstorms.
- Radio, optic (UV and IC) and soft energy gamma-radiation were registered.

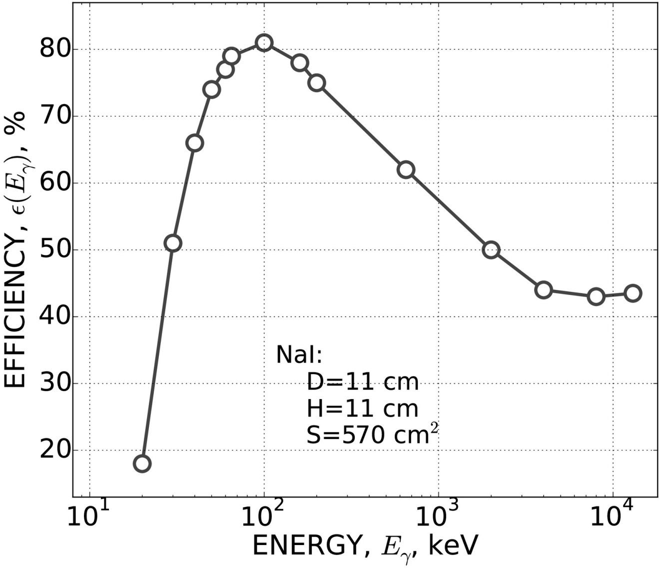
EFFICIENCY, $\epsilon(E_\gamma)$, %
ENERGY, E_γ, keV
NaI:
D=11 cm
H=11 cm
S=570 cm^2
80
70
60
50
40
30
20
10^1
10^2
10^3
10^4

Figure 1

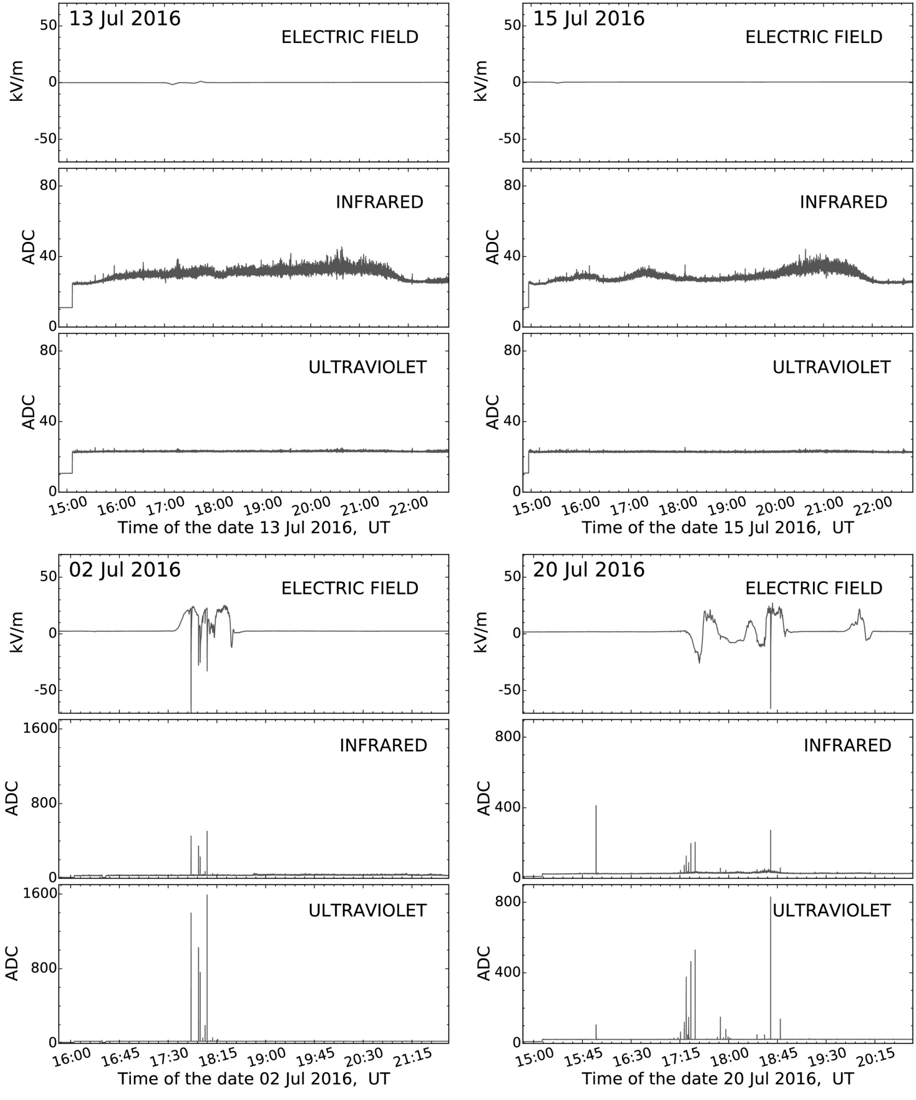
13 Jul 2016
ELECTRIC FIELD
kV/m
INFRARED
ADC
ULTRAVIOLET
ADC
Time of the date 13 Jul 2016, UT
15 Jul 2016
ELECTRIC FIELD
kV/m
INFRARED
ADC
ULTRAVIOLET
ADC
Time of the date 15 Jul 2016, UT
02 Jul 2016
ELECTRIC FIELD
kV/m
INFRARED
ADC
ULTRAVIOLET
ADC
Time of the date 02 Jul 2016, UT
20 Jul 2016
ELECTRIC FIELD
kV/m
INFRARED
ADC
ULTRAVIOLET
ADC
Time of the date 20 Jul 2016, UT

Figure 2

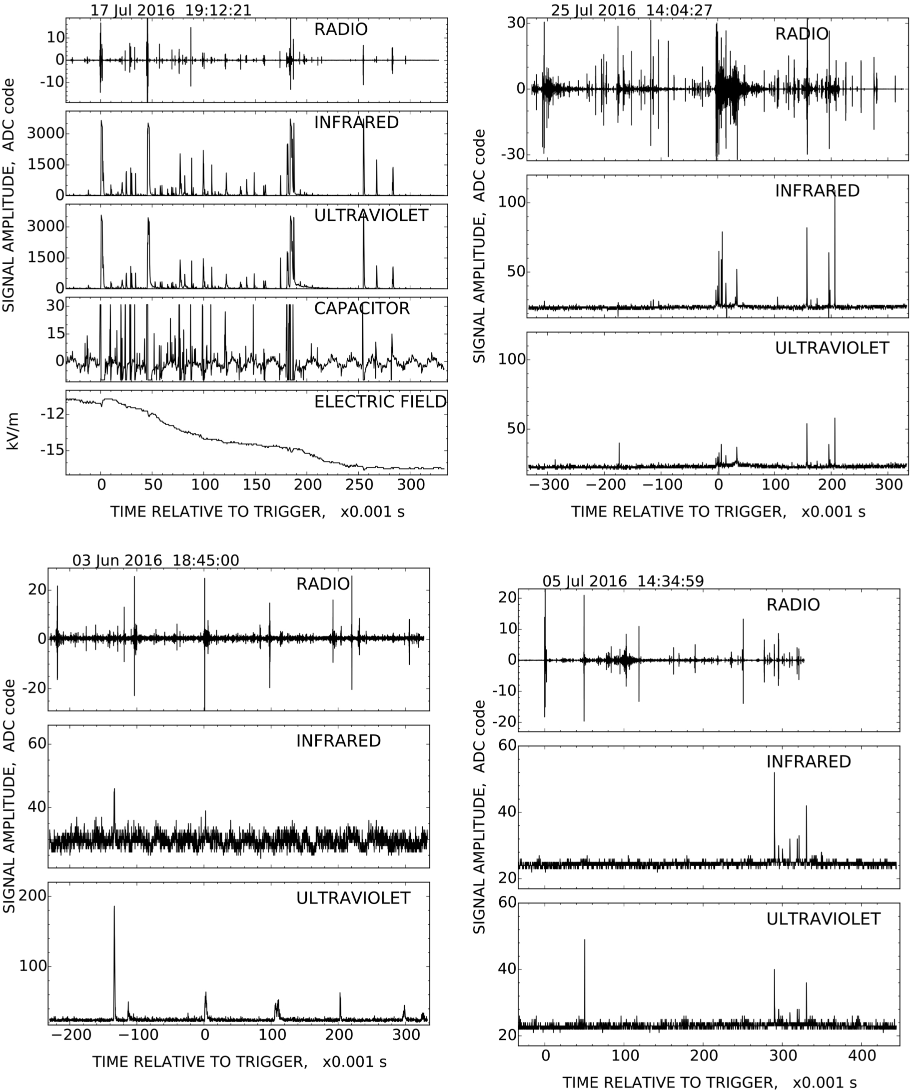
17 Jul 2016 19:12:21
RADIO
INFRARED
ULTRAVIOLET
CAPACITOR
ELECTRIC FIELD
SIGNAL AMPLITUDE, ADC code
kV/m
TIME RELATIVE TO TRIGGER, x0.001 s
25 Jul 2016 14:04:27
RADIO
INFRARED
ULTRAVIOLET
SIGNAL AMPLITUDE, ADC code
TIME RELATIVE TO TRIGGER, x0.001 s
03 Jun 2016 18:45:00
RADIO
INFRARED
ULTRAVIOLET
SIGNAL AMPLITUDE, ADC code
TIME RELATIVE TO TRIGGER, x0.001 s
05 Jul 2016 14:34:59
RADIO
INFRARED
ULTRAVIOLET
SIGNAL AMPLITUDE, ADC code
TIME RELATIVE TO TRIGGER, x0.001 s

Figure 3

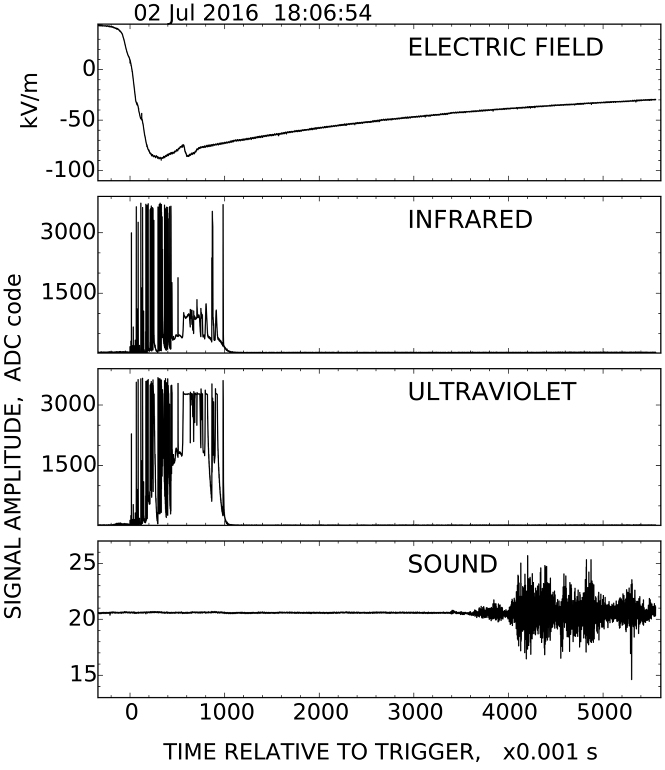
02 Jul 2016 18:06:54
ELECTRIC FIELD
kV/m
0
-50
-100
INFRARED
3000
1500
ULTRAVIOLET
3000
1500
SOUND
25
20
15
SIGNAL AMPLITUDE, ADC code
0
1000
2000
3000
4000
5000
TIME RELATIVE TO TRIGGER, x0.001 s

Figure 4

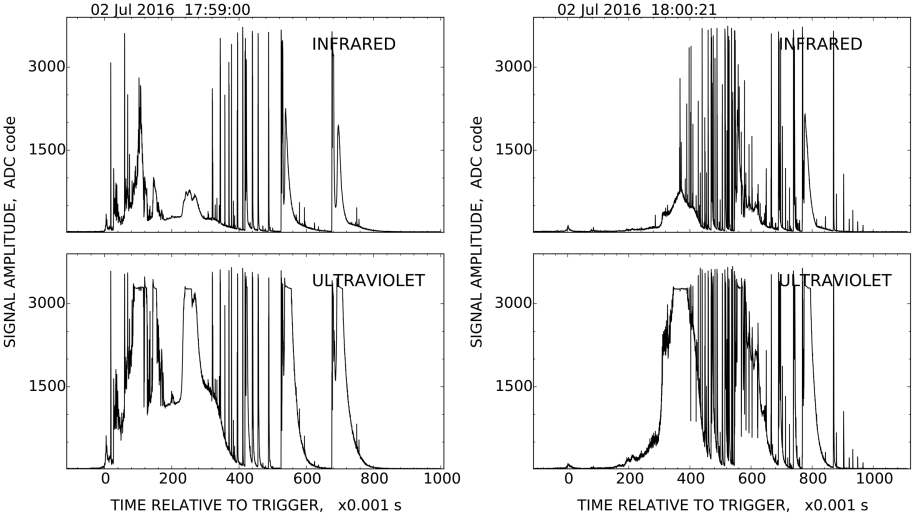

02 Jul 2016 17:59:00
02 Jul 2016 18:00:21
INFRARED
ULTRAVIOLET
INFRARED
ULTRAVIOLET
SIGNAL AMPLITUDE, ADC code
SIGNAL AMPLITUDE, ADC code
3000
1500
3000
1500
3000
1500
3000
1500
0
200
400
600
800
1000
0
200
400
600
800
1000
TIME RELATIVE TO TRIGGER, x0.001 s
TIME RELATIVE TO TRIGGER, x0.001 s

Figure 5

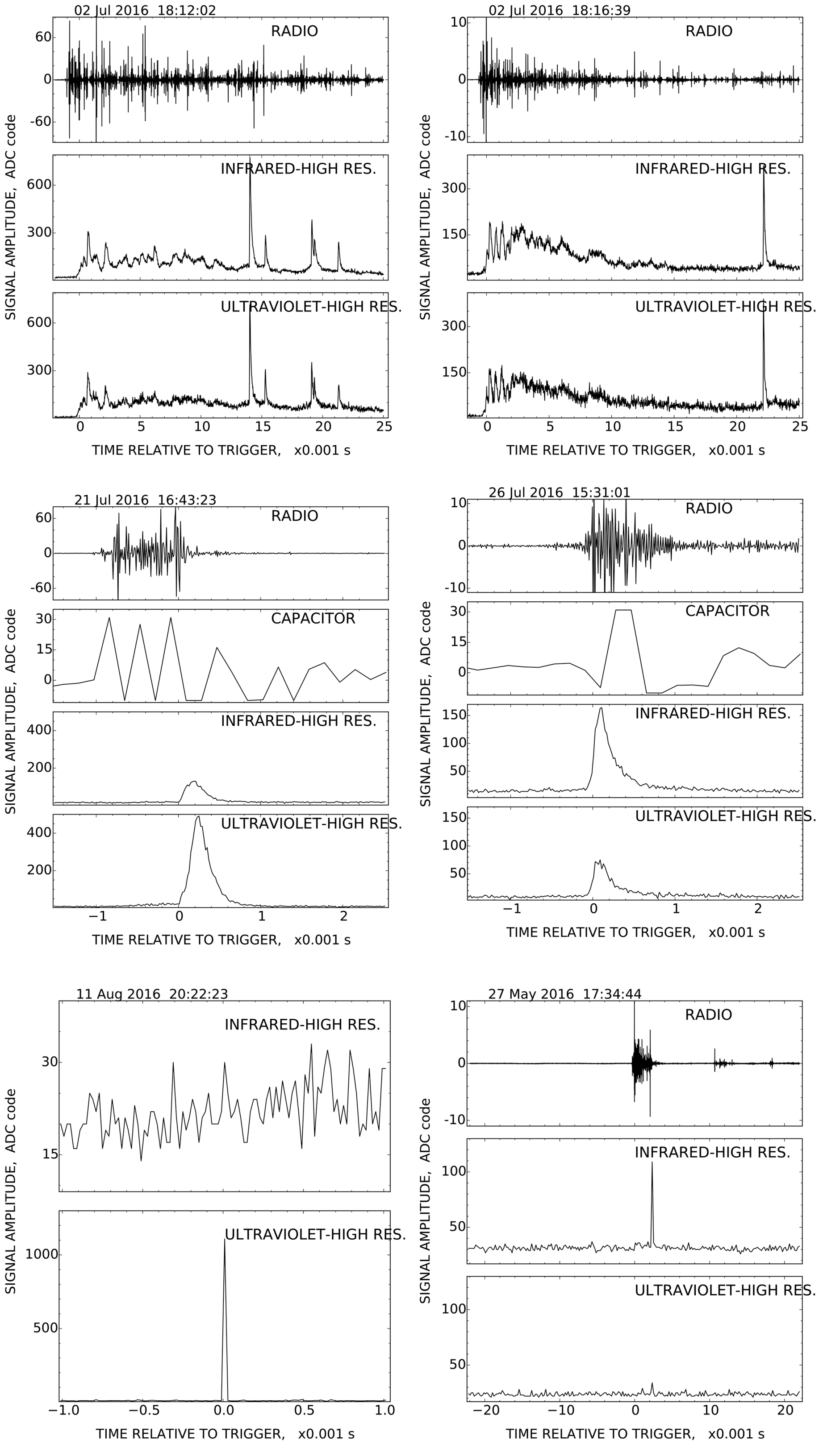
02 Jul 2016 18:12:02
RADIO
INFRARED-HIGH RES.
ULTRAVIOLET-HIGH RES.
SIGNAL AMPLITUDE, ADC code
TIME RELATIVE TO TRIGGER, x0.001 s
02 Jul 2016 18:16:39
RADIO
INFRARED-HIGH RES.
ULTRAVIOLET-HIGH RES.
SIGNAL AMPLITUDE, ADC code
TIME RELATIVE TO TRIGGER, x0.001 s
21 Jul 2016 16:43:23
RADIO
CAPACITOR
INFRARED-HIGH RES.
ULTRAVIOLET-HIGH RES.
SIGNAL AMPLITUDE, ADC code
TIME RELATIVE TO TRIGGER, x0.001 s
26 Jul 2016 15:31:01
RADIO
CAPACITOR
INFRARED-HIGH RES.
ULTRAVIOLET-HIGH RES.
SIGNAL AMPLITUDE, ADC code
TIME RELATIVE TO TRIGGER, x0.001 s
11 Aug 2016 20:22:23
INFRARED-HIGH RES.
ULTRAVIOLET-HIGH RES.
SIGNAL AMPLITUDE, ADC code
TIME RELATIVE TO TRIGGER, x0.001 s
27 May 2016 17:34:44
RADIO
INFRARED-HIGH RES.
ULTRAVIOLET-HIGH RES.
SIGNAL AMPLITUDE, ADC code
TIME RELATIVE TO TRIGGER, x0.001 s

Figure 6

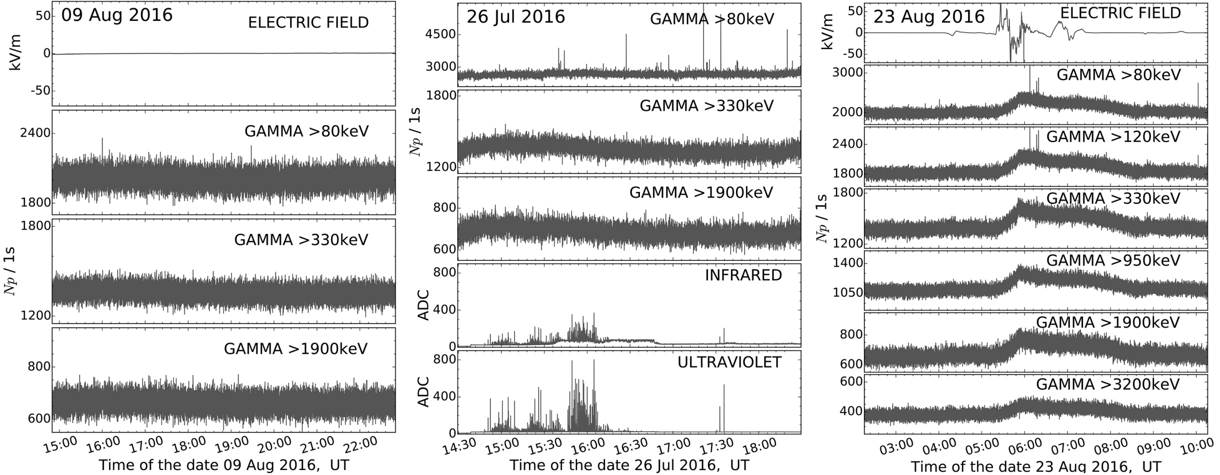
09 Aug 2016
ELECTRIC FIELD
kV/m
50
0
-50
GAMMA >80keV
2400
1800
GAMMA >330keV
1800
1200
Np / 1s
GAMMA >1900keV
800
600
15:00
16:00
17:00
18:00
19:00
20:00
21:00
22:00
Time of the date 09 Aug 2016, UT
26 Jul 2016
GAMMA >80keV
4500
3000
GAMMA >330keV
1800
1200
Np / 1s
GAMMA >1900keV
800
600
INFRARED
ADC
800
400
0
ULTRAVIOLET
ADC
800
400
0
14:30
15:00
15:30
16:00
16:30
17:00
17:30
18:00
Time of the date 26 Jul 2016, UT
23 Aug 2016
ELECTRIC FIELD
kV/m
50
0
-50
GAMMA >80keV
3000
2000
GAMMA >120keV
2400
1800
GAMMA >330keV
1800
1200
Np / 1s
GAMMA >950keV
1400
1050
GAMMA >1900keV
800
600
GAMMA >3200keV
600
400
03:00
04:00
05:00
06:00
07:00
08:00
09:00
10:00
Time of the date 23 Aug 2016, UT

Figure 7

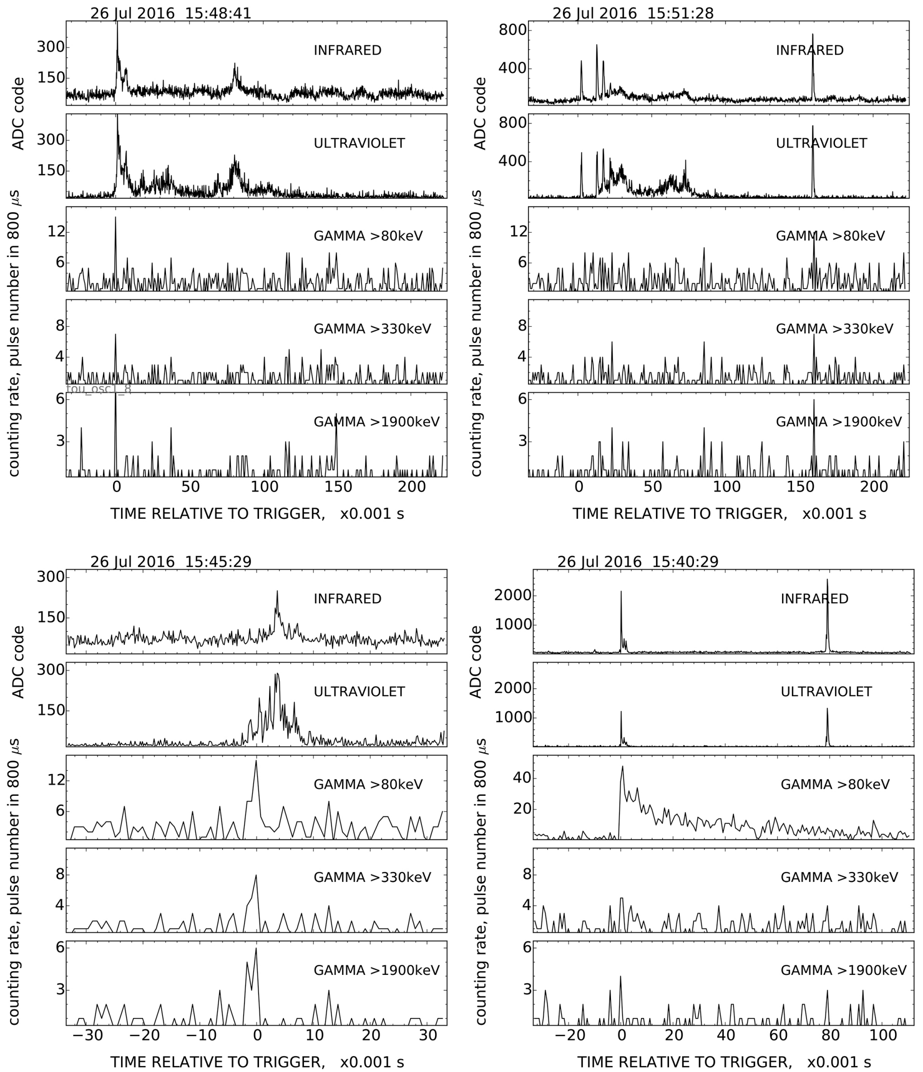
26 Jul 2016 15:48:41
26 Jul 2016 15:51:28
26 Jul 2016 15:45:29
26 Jul 2016 15:40:29
INFRARED
ULTRAVIOLET
GAMMA >80keV
GAMMA >330keV
GAMMA >1900keV
ADC code
counting rate, pulse number in 800 μs
TIME RELATIVE TO TRIGGER, x0.001 s

Figure 8